

## ON THE NUMERICAL COMPUTATION OF POINCARÉ MAPS

M. HENON

C.N.R.S., Observatoire de Nice, 06300 Nice, France

Received 8 February 1982

This note describes a method for finding simply and accurately the intersections of a numerically integrated trajectory with a surface of section.

The purpose of this note is to describe a trick which greatly facilitates the numerical computation of a Poincaré map in a dynamical system. This trick is simple, yet it does not seem to be widely known. It works quite well in practice: I have used it for a number of years without any problem.

We consider an autonomous dynamical system defined by  $N$  simultaneous differential equations:

$$\begin{aligned} \frac{dx_1}{dt} &= f_1(x_1, \dots, x_N), \\ &\dots \\ \frac{dx_N}{dt} &= f_N(x_1, \dots, x_N). \end{aligned} \quad (1)$$

A solution can be represented by a curve, or *trajectory*, in an  $N$ -dimensional phase space  $(x_1, \dots, x_N)$ . A frequently used technique consists in considering the successive intersections of the trajectory with a *surface of section*  $\Sigma$ , which in general is an  $(N-1)$ -dimensional subset of the phase space, defined by an equation

$$S(x_1, \dots, x_N) = 0. \quad (2)$$

The dynamical system (1) defines then a mapping of  $\Sigma$  on itself, known as a *Poincaré map*. The study of this mapping is often simpler and more illuminating than the study of the trajectories themselves.

In most cases, the Poincaré map is not given by explicit equations; it is defined implicitly by (1) and (2). In order to find the image of a point  $P$  of  $\Sigma$ , one must follow the trajectory emanating from that point until it intersects  $\Sigma$  again. We are thus confronted with two practical problems: (i) integrate numerically the differential equations (1) of the trajectory; (ii) detect and compute its intersections with  $\Sigma$  defined by (2).

The first problem has been intensively studied and can be considered as completely solved: nowadays one can choose among a number of excellent integration algorithms, with which a trajectory can usually be followed with high accuracy. The second problem, however, seems to have been neglected, perhaps because it was considered as trivial. As a result, and paradoxically, it is often at this stage that the largest computational error occurs.

The usual technique is to integrate, i.e. to obtain a sequence of *integration points* on the trajectory, and to evaluate  $S$  given by (2) at each point until a change of sign is detected. This means that the surface of section has been crossed; the intersection point is then found by interpolation. Here a choice must be made. One can do a crude linear interpolation between the last two integration points; this method is simple but produces an error which will be unacceptable in many cases. Or one can use higher-order interpolation formulas; but this requires a more

complex program, and the storage of a number of previous integration points. Even in that case, some error will be introduced.

One way out of this difficulty consists in arranging the integration scheme in such a way that one integration point lies exactly on  $\Sigma$ . The need for interpolation, and the attendant errors, are then entirely eliminated. We show now how this can be achieved. The only requirement will be that the integration scheme should allow independent time steps, i.e. each new time step can be computed independently of the preceding ones. This requirement is met, for instance, by Runge-Kutta and extrapolation algorithms; but predictor-corrector algorithms are eliminated.

We consider first the case where (2) has the simple form

$$x_i - a = 0, \quad (3)$$

where  $a$  is a constant; this particular form is the one most frequently encountered in practice. By a permutation of coordinates we can bring this to the form

$$x_N - a = 0. \quad (4)$$

We observe now that if the surface of section were defined by a condition on the independent variable  $t$ , of the form

$$t - a = 0, \quad (5)$$

it would be trivially easy to obtain an integration point on it, merely by choosing the appropriate time step. Our problem is that  $x_N$  in (4) is a dependent variable; therefore we cannot specify in advance its variation over one integration step. This observation gives us the key: simply rearrange the differential system in such a way that  $x_N$  becomes the independent variable! This is done by dividing the  $(N - 1)$  first equations in (1) by the last one, and inverting the last equa-

tion:

$$\begin{aligned} \frac{dx_1}{dx_N} &= \frac{f_1}{f_N}, \\ &\vdots \\ \frac{dx_{N-1}}{dx_N} &= \frac{f_{N-1}}{f_N}, \\ \frac{dt}{dx_N} &= \frac{1}{f_N}. \end{aligned} \quad (6)$$

$t$  has now become a dependent variable. The right-hand sides depend now on the independent variable  $x_N$ , but this is of no concern.

The practical procedure is as follows. We integrate the system (1) until a change of sign is detected for the quantity  $S = x_N - a$ . We shift then to the system (6). Using either the last computed point or the previous one as initial point\*, we integrate (6) for *one step*, taking as integration step

$$\Delta x_N = -S. \quad (7)$$

This brings us at once exactly on the surface of section!.

After having noted the coordinates of the point, we revert to the system (1) for the continuation of the integration†.

The only error in this procedure is the integration error for the system (6). This is usually of the same order as the integration error for one step of the system (1), and therefore it is negligible compared to the total integration error.

The actual coding is quite simple. It is not even necessary to write separately the equations (6): the two systems (1) and (6) can be merged into a single form. If we define  $\tau$  as the current

\*The use of the last point produces a slightly simpler program; the use of the previous point reduces slightly the total integration error. This choice is not critical.

†One might have the idea of abandoning the system (1) altogether and using only the equivalent system (6). This does not work, however, because (6) is singular for the zeros of  $f_N$ ; and there exists at least one such zero between any two intersections of the surface of section.

independent variable, and

$$K = \frac{dt}{d\tau}, \quad (8)$$

then (1) and (6) are two particular cases of the general form

$$\begin{aligned} \frac{dx_1}{d\tau} &= Kf_1, \\ &\vdots \\ \frac{dx_N}{d\tau} &= Kf_N, \\ \frac{dt}{d\tau} &= K, \end{aligned} \quad (9)$$

obtained by taking respectively  $K = 1$  and  $K = 1/f_N$ .

We consider now the general case where the equation (2) of the surface of section is arbitrary. We introduce an additional variable

$$x_{N+1} = S(x_1, \dots, x_N), \quad (10)$$

and we add the corresponding differential equation to the system (1):

$$\frac{dx_{N+1}}{dt} = f_{N+1}(x_1, \dots, x_N), \quad (11)$$

with

$$f_{N+1} = \sum f_i \frac{\partial S}{\partial x_i}. \quad (12)$$

We obtain a new system of order  $N + 1$ , with the surface of section defined by

$$x_{N+1} = 0. \quad (13)$$

This is of the form (3), and the above recipe can be applied.

Finally, the technique described here is also of interest when some of the functions  $f_i$  in (1), or some of their low-order derivatives, are discontinuous\* across an  $(N - 1)$ -dimensional subset of phase space defined by an equation

$$R(x_1, \dots, x_N) = 0. \quad (14)$$

The use of a high-order integration algorithm can then produce large errors whenever the "surface of discontinuity" (14) is crossed, because the algorithm implicitly assumes that all derivatives exist up to its order. The only remedy is to use an algorithm with independent time steps and to ensure that all points of intersection of the trajectory with the surface of discontinuity are integration points. Within each integration step, there is then no discontinuity and the algorithm gives accurate results.

In summary, the essence of the trick can be expressed as follows. A sophisticated machinery must in any case be available for the numerical integration of the orbit; and it turns out that this machinery, with a slight modification, can also be used to solve the intersection problem at no extra cost.

## References

- [1] M. Hénon, L'évolution Initiale d'un Amas Sphérique, *Ann. Astrophys.* 27 (1964) 83-91.

\*An example of this situation is encountered in the simulation of a globular star cluster by a system of concentric shells [1]: whenever two shells cross, the acceleration of each of them suffers a finite discontinuity.

## A NEW TYPE OF PERIOD-DOUBLING BIFURCATIONS IN ONE-DIMENSIONAL TRANSFORMATIONS WITH TWO EXTREMA

Jean COSTE and Nelly PEYRAUD

*Laboratoire de Physique de la Matière Condensée, Parc Valrose, 06034 - Nice Cedex, France*

Received 25 June 1981

Revised 13 January 1982

We consider the iteration of a one-dimensional transformation  $x \rightarrow f(x, \lambda)$ , symmetrical with the origin, and with two (symmetrical) extrema. There exists a sequence of period-doubling bifurcations where period- $2^k$  cycles are created at parameter values  $\lambda_k$ , and which is not of the Feigenbaum type. We show that the  $\lambda_k$ 's sequence converge toward a limit value as a double exponential function of  $k$ .

### 1. Introduction

It is well known that a set of successive subharmonic bifurcations appears [1, 4] in many dissipative flows (forced V.d.P. oscillators, parametric pendulum, etc.) when some control parameter  $\lambda$  of the vector field is varied. Moreover, the same cascade, with the same geometric sequence of  $\lambda_i$ 's is observed when one iterates a non-invertible transformation of the interval into itself:  $x \rightarrow f(x, \lambda)$ . An example is the logistic transformation with

$$f(x, \lambda) = \lambda x(2a - x). \quad (1)$$

This is the celebrated Feigenbaum sequence [5] (or "F sequence") which, most strikingly, has universal properties.

We want to report here on a different sequence of period-doubling bifurcations (we call it the  $\Sigma$  sequence), which we have encountered in the numerical study of 5 ordinary differential equations describing a model of Rayleigh-Benard convection [6]. In this problem, we have associated a Poincaré map to the flow in the phase space of the 5 variable  $\{x_i\}$ , in the following way: we considered the successive crossings (at times  $i$ ) of an orbit with a particular plane  $\pi$ . We thus obtain a 4-dimensional mapping. However, numerical integration

shows that the flow is so strongly contracting that the mapping may be considered with a good approximation as uni-dimensional, namely of the form  $x_a(i+1) = f[x_a(i)]$ ,  $x_a$  being one of the 5 variables (this means that  $f$  is nearly independent of the  $x_{i \neq a}(i)$ 's). Moreover,  $f$ , which is not monotonic, must be symmetrical vs. the origin, this property reflecting the invariance of the hydrodynamic flow when one changes the sign of rotation of the rolls. Finally, we had a mapping whose graph exhibited two extrema (symmetrical vs. origin). This is the kind of mapping we want to consider here, in general. Typical such quadratic maps are  $x \rightarrow f(x, \lambda)$  with

$$f(x, \lambda) = \text{sign}(x)\{Q(x - a \text{sign}(x))^2 - \lambda\}, \quad (2a)$$

$$f(x, \lambda) = \lambda x(|x| - 2a) \quad (2b)$$

( $a$  and  $Q$  being given constants), whose graphs are sketched on fig. 1.

Let us consider a transformation 1a and start with a value  $\lambda = \lambda_0$  such that  $f(x, \lambda)$  has stable fixed points  $\alpha$  and  $\alpha'$ . Increasing  $\lambda$  from  $\lambda_0$ , the curves  $\Gamma$  and  $\Gamma'$  move as is pictured on figs. 1a and 1b. A set of Feigenbaum bifurcations is observed in each invariant region ( $x > 0$  and  $x < 0$ ) before  $\Gamma$  crosses the  $x$ -axis (provided  $Q$  and  $a$  are large enough). Then, for  $\lambda = \lambda_1$ ,  $\Gamma$  comes into contact with the 2nd diagonal.

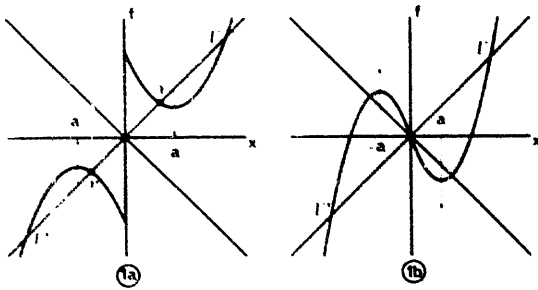


Fig. 1. Graphs of  $f(x, \lambda)$ . a)  $f(x, \lambda) = \text{sign}(x)\{Q(x - a \text{sign}(x))^2 - \lambda\}$ ; b)  $f(x, \lambda) = \lambda x(|x| - 2a)$ .

This implies (due to the symmetry vs. the origin) that the graph  $\Gamma_2$  of  $f_2 = f \circ f$  touches the first diagonal, creating by saddle node bifurcation a pair of symmetrical 2-cycles (one stable, the other one unstable): this is the first bifurcation of the  $\Sigma$  sequence.

Increasing  $\lambda$ ,  $\Gamma_2$  evolves exactly in the same way than in the case of a single maximum transformation, and the successive steps are pictured on fig. 2:  $C_2$  has its maximum stability when  $\Gamma_2$ 's maximum is on the first diagonal. Then, a pitchfork bifurcation occurs where  $C_2$

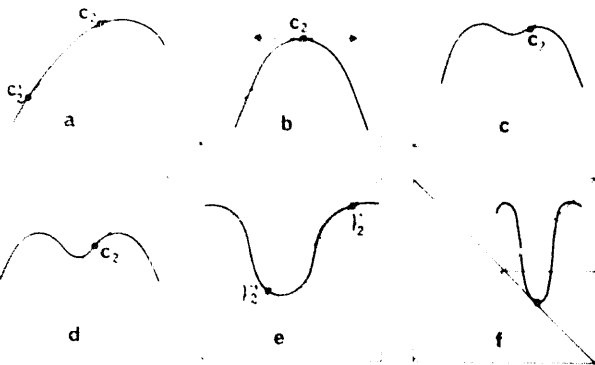


Fig. 2. Evolution of the graph  $\Gamma_2$  of  $f_2 = f \circ f$  when  $\lambda$  is increased in the neighbourhood of point  $(a, a)$ . (a) Creation of a pair of period-2 symmetrical cycles  $C_2, C_2'$  ( $C_2$  stable,  $C_2'$  unstable) by saddle-node bifurcation ( $\lambda = \lambda_1$ ); (b)  $C_2$  with maximum stability; (c) intermediary state between maximum of stability of  $C_2$  and the limit of stability of  $C_2$  cycle; (d) limit of stability of  $C_2$  cycle; (e) creation of two asymmetrical period-2 cycles  $\gamma_2, \gamma_2'$  by pitchfork bifurcation; (f) increasing  $\lambda$ , the minimum of  $\Gamma_2$  touches the 2nd diagonal, creating 2 period-4 cycles by saddle-node bifurcation ( $\lambda = \lambda_2$ ).

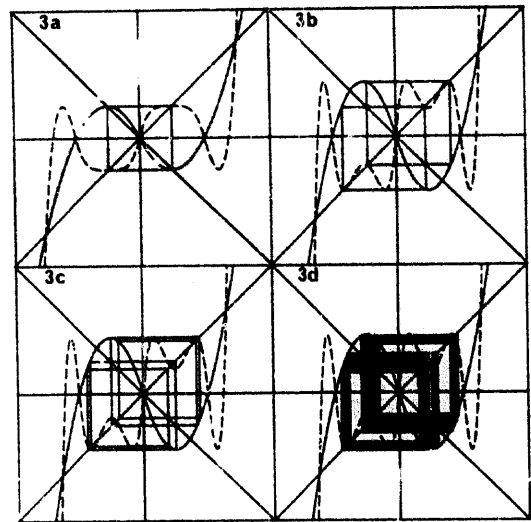


Fig. 3. Transformation (2b). Some periodic orbits encountered when increasing  $\lambda$ . a)  $\lambda = \lambda_1$ , Period-2 cycle  $C_2$  with maximum stability; b) two asymmetrical period-2 cycles  $\gamma_2, \gamma_2'$  issued from  $C_2$  by pitchfork bifurcation; c) first Feigenbaum period doubling of  $\gamma_2$  and  $\gamma_2'$ ; d) after the Feigenbaum cascade.

loses its stability to the benefit of two period-2, asymmetrical orbits (symmetrical from each other). Then, these last orbits suffer the Feigenbaum cascade of bifurcations. Later on  $\Gamma_2$  touches the 2nd diagonal (for  $\lambda = \lambda_2$ ), creating a period-4 stable cycle: this is the second bifurcation of the  $\Sigma$  sequence. We then consider  $\Gamma_4$ , and so on ...

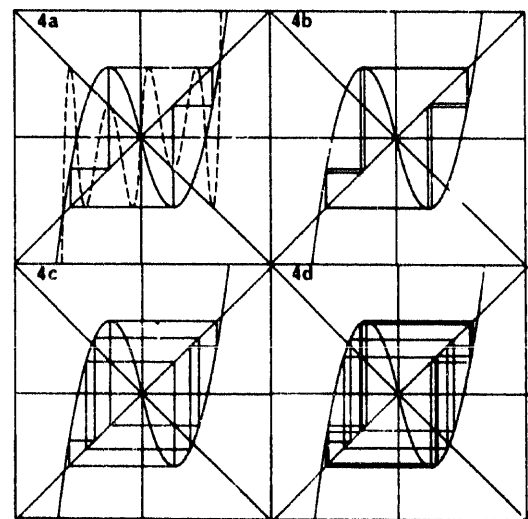


Fig. 4. Continuing fig. 3. a)  $\lambda = \lambda_2$ , period-4 cycle; b) asymmetrical period-4 cycle; c)  $\lambda = \lambda_3$ , period-8 cycle; d)  $\lambda = \lambda_4$ , period-16 cycle.

A set of symmetrical  $2^k$ -cycles are generated through successive saddle node bifurcations, for a set  $\{\lambda_k\}$  of control parameter values. Between two consecutive values  $\lambda_k$  and  $\lambda_{k+1}$  various period and aperiodic orbits are encountered, the first ones being the two asymmetrical  $2^k$ -cycles (produced by pitchfork bifurcation from the initial  $2^k$ -symmetrical cycle), followed by the sequence of their Feigenbaum sons.

The above scenario may not include the first step (namely the periodic orbits issued from the fixed points of  $f$ ). This is the case for transformations (2b). We have sketched on figs. 3 and 4 the later steps, described above.

## 2. Symbolic analysis of period- $2^k$ -cycles

First, we slightly modify the definition of  $\lambda_k$ 's sequence by considering the values  $\lambda'_k$  such that the cycles have maximum stability (instead of the bifurcation values). It is easily seen that any new  $\lambda'_k$  stays between former  $\lambda_k$  and  $\lambda_{k+1}$ , therefore the asymptotic behaviours of the 2 sequences are the same. The  $\lambda'_k$  sequence is chosen because it proves simpler to work on it (we relax the prime index in the following). Considering symmetrical mappings whose extrema are at  $x = \pm a$ , the new  $\lambda_k$  verify

$$f^{2^k}(a, \lambda_k) = a, \quad (3a)$$

or

$$f^{2^k-1}(a, \lambda_k) = -a. \quad (3b)$$

Let us also remark that, near the accumulation value  $\lambda_c$ , a point  $x$  has, in general, 2 or 3 inverses (see fig. 5).

Lying in one of the three following regions: region "0" ( $-a < x < a$ ), region "1" ( $x \geq a$ ), region "-1" ( $x \leq -a$ ). It is therefore natural to characterize an orbit's point  $x$  by a number  $a_i$  taking the value 0, 1 or -1 according to the region in which  $x$  stays. A periodic orbit is then

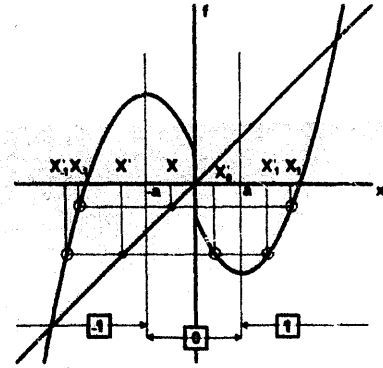


Fig. 5. A transformation when a point has 2 or 3 inverses. Labelling 3 regions on x-axis.

defined by a finite set of  $a_i$ 's, its "signature". We shall now show that the signature of a  $2^k$ -cycle belonging to our sequence contains only 2 values (namely  $a_i = \pm 1$ ) and that it is determined by a simple algorithm.

For  $\lambda = \lambda_2$  (period-2 cycle) we have the configuration of figs. 6a and 6b. We see that the cycle is defined by symmetrical points  $\{A_1, A_2\}$  (the successive images of point  $x = a$ ), giving the signature (1, -1). Increasing now  $\lambda$ ,  $A_1$  and  $A_2$  move toward  $\{A'_1, A'_2\}$  as shown on figs. 6a and 6b until the ordinates of  $A'_2$  reaches  $-a$ , which indeed happens if we assume a monotonic variation of  $f$  in  $|x| > a$ . Then,  $f^2(a) = -a$  and a period-4 cycle is generated (of maximal stability). But the symmetry vs. the origin demands that the "half cycle"  $A'_1, A'_2$  must be completed by its symmetrical counterpart  $A'_3, A'_4$ . Therefore, the signature of the  $2^2$ -cycle is obtained by taking the previous one (1, -1) and

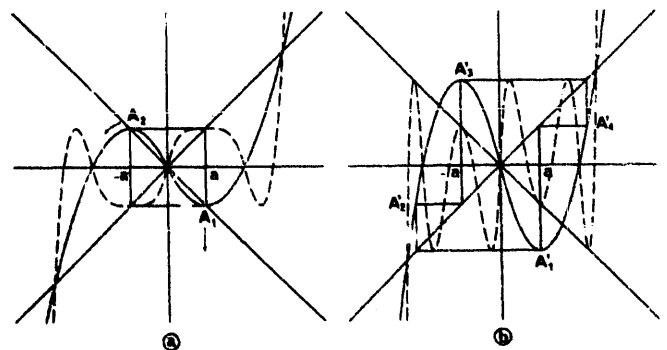


Fig. 6. Passing from period-2 cycle (a) to period-4 cycle (b).

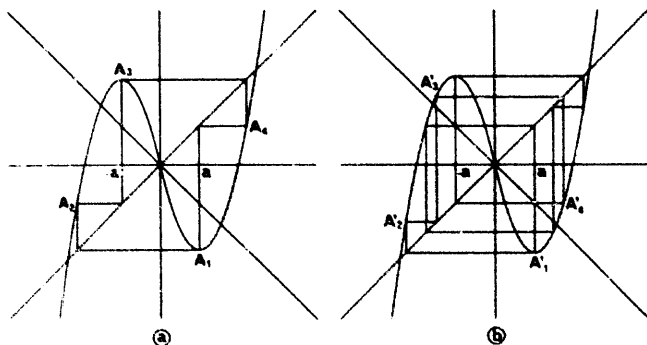


Fig. 7. Passing from period-4 cycle (a) to period-8 cycle (b).

adding its symmetrical, which gives  $(1, -1, -1, 1)$ . In the same way, fig. 7 shows the passage from a period-4 to a period-8 cycle, whose signature is  $(1, -1, -1, 1 | -1, 1, 1, -1)$  and so on. The procedure is always the following: increasing  $\lambda$  we deform the  $2^k$ -cycle until  $f^{2^k}(a) = -a$ , creating the "half  $2^{k+1}$ -cycle" and we obtain the complete  $2^{k+1}$ -cycle taking the symmetrical part of half cycle vs the origin. Moreover, we verify that we never get an orbit point in the "zero" region. Of course, this would not be true for a  $2^k$ -cycle which is not maximally stable, but its signature would be the same provided we consider only two regions, namely  $x > 0$  (region "1") and  $x < 0$  (region "-1").

### 3. The case of a piece-wise linear application

In this case an analytic study of the  $\lambda_k$ 's sequence can easily be done. Let us consider the transformation (2c) defined by

$$f \equiv \mu|x - \frac{1}{2} \text{sign}(x)| - \lambda \text{sign}(x), \quad (\mu > 1)$$

as shown on fig. 8, where  $\mu$  is fixed and  $\lambda$  is the bifurcation parameter.

This simple example will permit us to show the doubly exponential behaviour of the asymptotic  $\lambda_k$ 's sequence as a function of  $k$ . We have here a degenerate case: the  $2^k$ -cycles exist but are unstable and they are still defined by:  $f^{2^k-1}(\frac{1}{2}, \lambda_k) =$

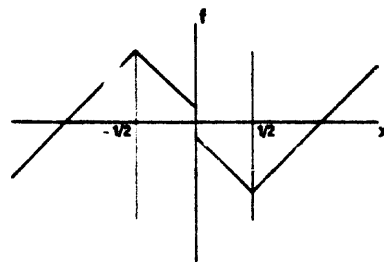
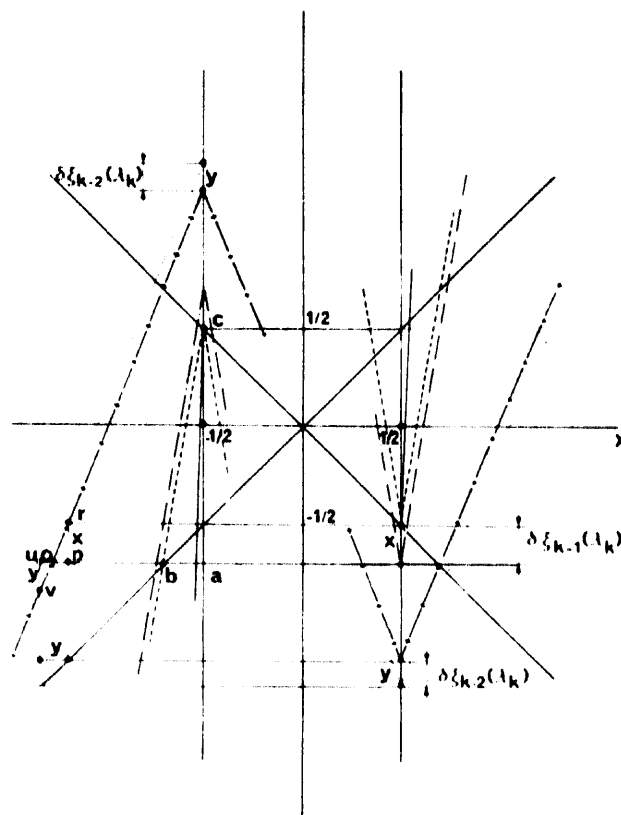


Fig. 8. Graph of transformation (2c).

Fig. 9. Graphs of some iterates of (2c) transformations in the neighbourhood of  $x = \pm \frac{1}{2}$ . —  $f^{2^k}(\lambda_{k+1})$ ; - - -  $f^{2^{k-1}}(\lambda_k)$ ; ·····  $f^{2^{k-2}}(\lambda_{k+1})$ ; + + + +  $f^{2^{k-3}}(\lambda_k)$ ; .....  $f^{2^{k-4}}(\lambda_{k+1})$ .

$-\frac{1}{2}$ . The graphs of  $f^{2^k}(x, \lambda_{k+1})$ ,  $f^{2^{k-1}}(x, \lambda_k)$ ,  $f^{2^{k-2}}(x, \lambda_{k+1})$ ,  $f^{2^{k-3}}(x, \lambda_k)$  and  $f^{2^{k-4}}(x, \lambda_{k+1})$  are sketched on fig. 9 in the vicinity of  $x = \pm \frac{1}{2}$ .

Let  $\xi_{k-1}(\lambda_k) = |f^{2^{k-1}}(\frac{1}{2}, \lambda_k)|$  (by definition  $\xi_{k-1}(\lambda_k) = \frac{1}{2}$ ). Going from  $\lambda_k$  to  $\lambda_{k+1}$  (or from a  $2^k$ -cycle to a  $2^{k+1}$ -cycle) we increase  $\lambda_k$  by  $\delta\lambda_k$  and  $\xi_{k-1}(\lambda_k)$  by  $\delta\xi_{k-1}(\lambda_k) = \xi_{k-1}(\lambda_{k+1}) - \xi_{k-1}(\lambda_k)$ . Inspection of triangle  $abc$  on fig. 9 shows that  $\mu_{k-1} = (1 + \delta\xi_{k-1})/\delta\xi_{k-1}$ , where  $\mu_{k-1} = |df^{2^{k-1}}/dx| = \mu^{2^{k-1}}$ ,

or  $\delta\xi_{k-1} = 1/(\mu_{k-1} - 1)$ . Now a variation  $\delta\xi_{k-1}(\lambda_k)$  of the minimum of  $f^{2^{k-1}}(x, \lambda_k)$  induces a variation  $\delta\xi_{k-2}(\lambda_k)$  of the minimum of  $f^{2^{k-2}}(x, \lambda_k)$  which is related to  $\delta\xi_{k-1}(\lambda_k)$  by  $\delta\xi_{k-1} = (\mu_{k-2} - 1) \delta\xi_{k-2}$  (see triangles *ouv*, *opr* on fig. 9). From that we obtain

$$\delta\xi_{k-1} = \frac{1}{\mu_{k-1} - 1} = (\mu_{k-2} - 1)(\mu_{k-3} - 1) \dots (\mu_2 - 1)(\mu - 1)\delta\lambda_k,$$

or

$$\delta\lambda_k^{-1} = \prod_{p=1}^{k-1} (\mu_p - 1).$$

Taking the logarithm of this equality (with  $\mu_1 = \mu$ )

$$\log \delta\lambda_k^{-1} = \sum_{p=1}^{k-1} \log \mu_p + \sum_{p=1}^{k-1} \log(1 - \mu_p^{-1}).$$

As  $k \rightarrow \infty$  the second sum obviously converges toward some constant, therefore we obtain in the large  $k$  limit

$$\lim_{k \rightarrow \infty} \delta\lambda_k^{-1} \approx \prod_{p=1}^{k-1} \mu_p \approx \mu^{2^k},$$

or

$$C = \lim_{k \rightarrow \infty} \frac{1}{k} \log \log \delta\lambda_k^{-1} = \log 2.$$

#### 4. Numerical study of a continuous transformation

We have studied transformations of the forms (1a) and (1b). Finding a numerical solution of the equation  $f^{2^{k-1}}(a, \lambda_k) = -a$  encounters a double difficulty: i) the convergence of the  $\lambda_k$ 's sequence is so strong that quadruple precision is needed in the computation. Nevertheless, the number of available bifurcations is usually not very large; ii) near the accumulation value  $\lambda_c$  the "average" derivative  $|df/dx|$  is large and this causes prohibitive numerical errors in the calculation of long period orbits (compare from

this point of view the  $\Sigma$  sequence relative to a (2a) transformation with  $Q=1$ , and the F sequence relative to logistic transformation (1): the accumulation associated with  $\Sigma$  sequence is larger than those associated with F sequence; therefore, the average  $|df/dx|$  is larger). A better precision is obtained by working on the inverse transformation (i.e. by solving equation  $f^{-2^{k-1}}(-a, \lambda_k) = a$ ). The correct labelling of successive inverses is easily derived from the signature of the  $2^k$ -cycles.

Analogous results have been obtained for transformations (2a) and (2b), and we present here those relative to (2a). We have sketched on fig. 10  $(1/k) \log \log \delta\lambda_k^{-1}$  as a function of  $k$  for several values of parameters  $a$  and  $Q$ .

Three comments can be done:

i) we verify that  $(1/k) \log \log \delta\lambda_k^{-1}$  goes to a limit  $C$  for large  $k$ . The accuracy is improved when  $f$  is such that the orbit points are localized

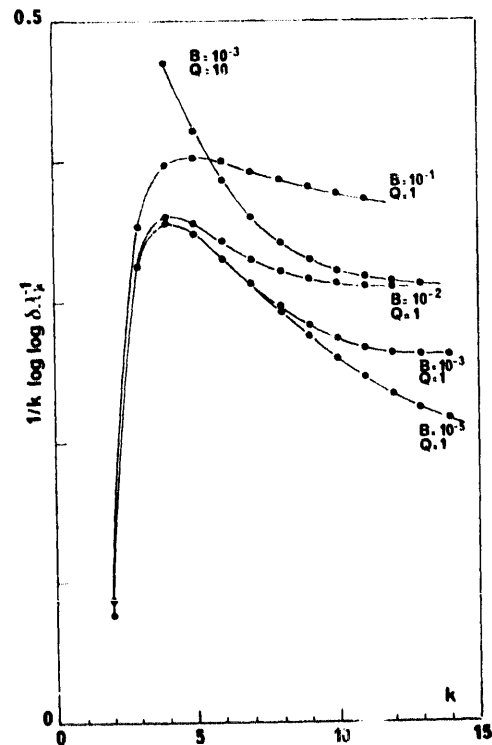


Fig. 10. Graph of  $(1/k) \log \log \delta\lambda_k^{-1}$  as a function of  $k$  for transformation (2a) and for several values of parameters  $B$  and  $Q$  (numerical results).



in an interval where  $|df/dx|$  is not too large. Indeed, we get then a moderate value of  $C$  and many iterations can be performed. This happens for small enough values of  $a$  and  $Q$ ;

ii) the constant  $C$  is not universal for quadratic maps: it obviously depends on the transformation parameters;

iii) when  $a = 0$  we get a transformation whose graph is piecewise monotonic in  $x > 0$  and  $x < 0$ . It is interesting to notice that such a transformation has been studied by Arneodo, Couillet, Tresser [7] as the Poincaré map of a 3-dimensional flow. Then, period- $2^k$ -cycles of the map were associated with stable homoclinic orbits of the flow (the origin being the homoclinic point). In the case of a quadratic map the  $\Sigma$  sequence reduces to the  $F$  sequence [7]. Our numerical results indicate that  $C$  decreases markedly as  $a \rightarrow 0$ . However, it is difficult to verify that  $\lim_{a \rightarrow 0} C = 0$ , and that the  $\Sigma$  sequence approaches a geometrical one: indeed, as  $a$  goes to zero, one needs more and more iterates for reaching the asymptotic value of  $(1/k) \log \log \delta \lambda_k^{-1}$ . We conclude by making the following remarks: We have considered a set of successive saddle-node bifurcations occurring when

one varies some parameter  $\lambda$  of a particular type of transformations. Our interest was driven on it by the study of a flow associated with ordinary differential equations. Moreover, the first  $2^k$ -cycles of our  $\Sigma$  sequence exist in relatively large "windows" of the bifurcation parameter, making them easy to observe in the presence of random fluctuations. Let us also notice that such sequences of period-doubling bifurcations\* could be detected in experimental devices with the help of characteristic signature of the cycles. Now the bifurcations'  $\Sigma$  sequence is only a particular one. Clearly, it would be interesting to study different sequences (an example could be the appearance of successive  $RL^m$  cycles in a one maximum-transformation) and to see if the associated  $\lambda_k$ 's sequence still converge toward their limit according to a doubly exponential law.

## References

- [1] V. Franceschini, *J. Stat. Phys.* 22 (1980) 397.
- [2] Y. Pomeau, *Lectures Notes in Physics* (Springer) 71 (1977) 337.
- [3] P. Couillet, C. Tresser and A. Arneodo, *Phys. Lett.* 72A (1979) 268.
- [4] C. Tresser, Thesis, Nice University (1981).
- [5] M.J. Feigenbaum, *J. Stat. Phys.* 19 (1978) 25.
- [6] J. Coste and N. Peyraud, *Phys. Lett.* 84A (1981) 17.
- [7] A. Arneodo, P. Couillet and C. Tresser, *Phys. Lett.* 81A (1981) 197.

\*Since this article was submitted for publication, Dr. Collet told me that this kind of period-doubling bifurcations was found at the same time but in a different context by W.A. Beyer and P.R. Stein, whose work has been submitted for publication.